Origins of the Solvent Effect on the Propagation Kinetics of Acrylic Acid and Methacrylic Acid

Isa. Degirmenci,[1] Tugba Furuncuoglu Ozaltın,[2] Ozlem Karahan,[2] Veronique Van Speybroeck,[3] Michel. Waroquier,[3] Viktorya Aviyente[4]

[1]ARC Centre of Excellence for Free-Radical Chemistry and Biotechnology, Research School of Chemistry, Building 35, Australian National University, Canberra ACT 0200, Australia
[2]Department of Chemistry, Boğaziçi University, 34342, Bebek, Istanbul, Turkey
[3]Center for Molecular Modeling, Ghent University-Member of the QCMM-Alliance Ghent-Brussels, Technologiepark 903, 9052 Zwijnaarde, Belgium
Correspondence to: V. Aviyente (E-mail: aviye@boun.edu.tr)

Received 14 August 2012; accepted 18 January 2013; published online 20 February 2013
DOI: 10.1002/pola.26589

ABSTRACT: In this study, the relative rate of polymerization of acrylic acid (AA) versus methacrylic acid (MAA) and the effect of water on the polymerization kinetics are investigated within a combined static and molecular dynamics set of computational tools. Experimentally the relative rate of propagation of AA versus MAA is around 35 in bulk and 31 in water. Classical Molecular Dynamics calculations have been carried out to determine the location of the solvent molecules in the proximity of the dimeric poly(AA) and poly(MAA) units. A combined implicit/explicit solvent model was used for the evaluation of the kinetics of the dimeric polymer chains. We show that the rate acceleration of both polymers in water is mainly due to entropic rather than electrostatic effects and is in agreement with experimental findings. Moreover the slower propagation rate of MAA versus AA is ascribed to additional steric effects present in MAA due to the methyl group at the α position of the monomer. Among the functionals used, the M06-2X/6-311+G(3df,2p)//B3LYP/6-31+G(d) methodology reproduces the experimental rate constants quantitatively the best. © 2013 Wiley Periodicals, Inc. J. Polym. Sci., Part A: Polym. Chem. **2013**, *51*, 2024–2034

KEYWORDS: acrylic acid; kinetics; methacrylic acid; propagation; solvent effect

INTRODUCTION Water-soluble polymers are of high importance, finding widespread applications in hydrogels, flocculants, thickeners, coatings, and have adhesion characteristics.[1,2] Pulsed-laser polymerization in conjunction with size-exclusion chromatography has been carried out to monitor the influence of solvents on the propagation kinetics of free radicals.[3,4] The effect of solvent on the kinetics of the free radical polymerization (FRP) of acrylates, methacrylates and other vinylic monomers has been investigated.[5] It is known that rate enhancement or retardation depends not only on the monomer structure and the nature of the solvent separately but also on the specific type of interactions between the reacting species and the solvent.[6]

It is known that the propagation rate coefficients for styrene and methyl methacrylate (MMA) in a wide variety of solvents (acetonitrile, dimethyl formamide, anisole, methyl isobutyrate, bromobenzene, benzene and 1,2-dichloroethane) only change mostly by 10% (see review of S. Beuermann and references cited therein).[5] Conversely, certain solvents, such as benzyl alcohol,[7,8] dimethylsulfoxide,[7,8] *N*-methylpyrrolidinone,[7,8] 2,6-dithiaheptane,[9] and 1,5-dithiacyclooctane[9] induce a significant increase in k_p. In many cases hydrogen bonding is responsible for this observed rate acceleration. The usage of alcohols as solvents in the FRP of acrylates has caused a rate enhancement which was attributed to a decrease in electron density around the C=C bond of the monomer due to the hydrogen bonding between the solvent and the oxygen atom of carbonyl group.[10] The rate of propagation, k_p, of MMA in benzyl alcohol has been reported to increase by almost one order of magnitude as compared to bulk polymerization.[7,8]

When there are no specific interactions between the monomer and the solvent, a correlation between the propagation rate constant $k_{p,}$ the size of the solvent molecules and the monomer has been established.[5] Thus, one expects an increase in the propagation rate constant when the solvent is larger in size than the monomer. When the solvent size is smaller than the monomer, the propagation rate constant decreases. These results were explained by a change in local concentration of the monomer around the growing chain end: a larger solvent size leads to an increase in local

monomer concentration around the growing chain end increasing the propagation rate constant and vice-versa.[5]

For the FRP of styrene (in ethanol, methanol, toluene, ethylbenzene), methacrylic acid (MAA) (in methanol, tetrahydrofuran, 2-propanol, toluene, and acetic acid), methyl methacrylate (in methanol, ethyl acetate, ethanol, toluene, 2-butanone), and butyl acrylate (in toluene, tetrahydrofuran) it was shown that the propagation rate constant k_p is invariant with monomer concentration.[11–17] Increase in k_p with dilution of monomer concentration was observed for acrylamide (AM) and methacrylamide (MAM) derivatives,[18–21] acrylic acid (AA) and MAA.[12,15,22–28] This strong solvent effect was attributed to dimerization,[18,21] or to local monomer concentrations at the radical site being different from the overall monomer concentration.[27] These studies have revealed the fact that polar monomers, that are capable of forming hydrogen bonds, are affected substantially by the solvent.[29–32] When the bulky system is diluted, the propagation rate constant k_p of MAA and AA has been reported to increase by at least one order of magnitude. This change was reflected in an increase in the Arrhenius pre-exponential factor, due to the disorder created by strong hydrogen bonding between the growing species and water molecules.[23,33–35]

In the last two decades quantum chemical studies on the FRP of vinyl monomers,[10,36–53] acrylate and methacrylate derivatives,[36,37,48,54–66] and their copolymerization [57,58,60,67] have been carried out. In these studies at least two units were considered to mimic the growing polymer chain and to obtain reliable kinetic results. Implementation of the solvent by a polarizable continuum model (PCM) has lead to serious underestimation of the experimentally obtained propagation rate constant in the case of ethyl α-hydroxymethacrylate.[68,54] Usage of the PCM methodology, in bulk for methyl acrylate (MA) and methyl methacrylate (MMA) has lead to a very good qualitative agreement with the experimentally observed trends.[69] Thicket and Gilbert [65] have monitored the effect of the solvent on the propagation reaction of the monomers: a decrease in the activation barrier was attributed to a greater resonance stabilization of the transition state in a polar medium.

Recently, the COSMO-RS methodology has yielded promising results to simulate the solvent effect.[46,69] Coote et al. have obtained highly accurate propagation rate constants for MA and vinyl acetate by using the thermodynamic cycle in which G3(MP2)-RAD calculations in the gas phase are corrected by the solvation energies obtained from COSMO-RS. [45,46,70,71] The latter have used the G3(MP2)-RAD methodology that approximates CCSD(T) calculations with a large triple-ζ basis from calculations with a double-ζ basis set, via basis set corrections carried out at the R(O)MP2 level of theory.[70,71] They calculated the rate coefficients and Arrhenius parameters with this composite method for dimer models and have corrected their gas phase results by computing solution phase calculations with the COSMO-RS method.[72–74] Warshel and coworkers have carried out a comparative study between continuum, explicit and mixed implicit/explicit solvation models in the context of phosphate hydrolysis.[75] Some of us have used successfully the mixed implicit/explicit solvation model to study the propagation reaction of MMA, n-isopropylacrylamide, acrylamide (AM), and methacrylamide (MAA).[56,62,66] In these studies, the experimentally observed head to tail propagation[76] which is assumed to be the most favorable mode of attack was proven by theoretical methods.[51]

Thus, the elucidation of the solvent effects on the reaction kinetics of FRP is of utmost importance and quantum chemical calculations can give insight at the molecular level. In this study, we focus on acrylic and MAA and we compare the geometrical features of the propagating species in bulk and in solution to unravel the role of water on the propagation rate constants of AA and MAA. The propagation ratio of AA/MAA which is around 35 in bulk, lowers slightly to 31 in water[25,27] and it is the goal of this study to understand the mode of acceleration of the propagation of the FRP of AA and MAA by a protic and polar medium.

Computational Procedure

The FRP of a monomer starts with the generation of free radicals from the initiator (the non-radical species).

$$\mathrm{I} \xrightarrow{k_d} \mathrm{R}\bullet \qquad (\text{initiation})$$

Addition of R·-the methyl (CH_3·) radical for unimeric species-to a monomer yields a backbone with three carbon atoms. This type of approach—addition of CH_3 to the carbon–carbon double bond (C=C) by the aid of quantum chemical tools—has already been used previously.[10,38–43,52,53,77,78] The unimeric radical then adds to the monomer to generate the propagating polymer chain (propagation reaction; Scheme 1). In this study we systematically located the transition states for both unimeric and dimeric radical models, to evaluate the influence of the length of the radical chain on the propagation kinetics.

The B3LYP methodology combined with 6-31+G(d) basis set within the Gaussian 03 program package[79] has been used as a cost effective and accurate method for geometry optimizations.[80] COSMO-RS calculations were performed with ADF.[81] The energetics and kinetics in vacuum and in solution have been evaluated with the MPWB1K/6-311+G(3df,2p)//B3LYP/6-31+G(d), M05-2X/6-311+G(3df,2p)//B3LYP/6-31+G(d), and M06-2X/6-311+G(3df,2p)//B3LYP/6-31+G(d) methodologies to further refine the energy at another level of theory. The MPWB1K method was chosen because it has been proven to be successful for describing thermochemistry, reaction kinetics, hydrogen bonding, and weak interactions.[60,82] This method has also been found to be successful

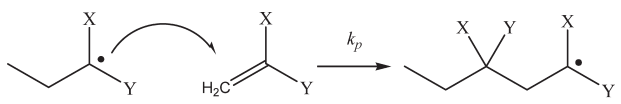

X=-H for AA and -CH_3 for MAA
Y=-COOH

SCHEME 1 Propagation of AA and MAA.

in studies concerning the FRP reactions of acrylates.[37,55,56,60,62,64,66] The M05-2X[83] and M06-2X[84] functionals have been chosen because they are recommended for thermochemistry, kinetics, and noncovalent interactions.[83,84] The M05-2X functional is further known to be successful for radical species.[37,85–95] According to Zhao and Truhlar, the M05-2X functional implicitly accounts for "medium-range" electron correlation because of the way it is parametrized, and this is sufficient to describe the dispersion interactions within many complexes.[84] These authors define "medium-range"correlation to be that found in complexes separated by about 5 Å or less.[96] The main intermolecular interactions in the species analyzed in this study are hydrogen bondings thus M05-2X and M06-2X functionals are expected to reproduce these interactions quite well. The conventional transition state theory is used to calculate the rate constants. The rate constant of a bimolecular reaction A + B → C is expressed[97] in terms of the molecular Gibbs free energy difference between the activated complex and the reactants (with inclusion of zero point vibration energies):

$$k_2 = \kappa \frac{kT}{h} \frac{\mathrm{RT}}{p^{\theta}} e^{-\Delta \mathrm{G}^{\ddagger}/\mathrm{RT}}$$

where R represents the universal gas constant and κ is the transmission coefficient which is assumed to be about 1 and p^{θ} is the standard pressure 10^5 Pa (1 bar).[98]

For implicit solvation, the effect of a polar environment was taken into account by use of the self-consistent reaction field theory, utilizing the integral equation formalism-PCM.[99–102] For the case where the solvent has been modeled explicitly and implicitly, the contribution resulting both from the explicit coordination with solvent molecules in the reactants and transition states and the one originating from the bulk solvent effect as in earlier publications have been considered.[75,103–106] In the latter case all gas phase geometries were re-optimized in polarizable continuum medium (PCM) with explicit water molecules (implicit/explicit solvation model) to access the effect of the solvent. The calculated free energy of solvation was corrected with the term RT ln (24.46) to take into account the unit transformation from 1 mol/L (g) to 1 mol/L (soln).[107] These structures were further used to calculate the solvation energies with the new generation method COSMO-RS.[72–74] All the energies reported in this study are in kcal/mol.

Classical MD simulations were performed on the dimers of poly(AA) and poly(MAA). The simulation box was composed of three dimeric chains and 250 water molecules, a solution with a density of 1 g/cm^3 having 9 wt % poly(AA/MAA). Each side of the cubic box was 20.2 Å. The box was constructed with the Amorphous Cell module of Accelrys Materials Studio suite of programs.[108] The COMPASS forcefield[109] was used with a cut-off distance of 10 Å, and a switching function with spline and buffer widths of 1.0 and 0.5 Å, respectively. The system was initially minimized with 5000 steps of conjugate gradients up to a convergence of 1 kcal/mol/Å. Then, periodic boundary conditions were imposed and MD simulations were performed in the NVT ensemble at 298 K using the Andersen thermostat as the temperature control method with a collision ratio of 1.0.[110] 200 ps equilibration run was followed by a production run of 1 ns. The time step was set to 1 fs and coordinates from the production stage were recorded every 1 ps for further analysis. The radial distribution functions analyzed in this study are based on 1000 snapshots.

RESULTS AND DISCUSSION

Propagation of AA and MAA in Vacuum

A conformational search was carried out for the monomers and the radicals at the B3LYP/6-31+G(d) level of theory. The s-*cis* geometry has the lowest energy for AA, while the s-*trans* conformer is preferred in case of MAA. Although the energy difference between s-*cis* and s-*trans* conformers is only 0.31 and 0.45 kcal/mol for AA and MAA respectively (Fig. 1), the rotational barrier between the s-*cis* and s-*trans* conformers of AA is 6.69 kcal/mol and that of MAA is 5.84 kcal/mol (Supporting Information Fig. S1). These results are consistent with previous theoretical studies on MA and MMA.[55] Notice that in both cases long range electrostatic interactions between the carbonyl oxygen and hydrogens stabilize these structures. In the case of MAA s-*trans* is preferred because of the bifurcation of the carbonyl oxygen between the hydrogens of the methyl group. A similar conformational study was performed for the radicals formed by addition of CH_3 radical to the monomers, as they may adopt either a *syn* or *anti* configuration (Fig. 1).

Racemo and meso dimeric radicals may be formed by attack of the most stable conformation of the radical (*syn*/*anti*) to the most stable conformation of the monomer (s-*cis*/s-*trans*) as schematically depicted in Scheme 2.

All the plausible combinations for the radical addition to the monomer were used giving rise to eight different transition states. For each of these transition structures a relaxed potential energy scan was carried out around the forming bond (Supporting Information Figs. S2 and S3); in this way the most stable transition state structures were located. The most stable structures for the unimeric and dimeric transition structures of **AA** and **MAA** are displayed in Figure 2.

In vacuum, the pro-racemo (syndiotactic) transition state of AA is preferred whereas the pro-meso (isotactic) attack is prefered for MAA as seen from Table 1, where the relative electronic energies are tabulated for the eight different transition structures of AA and MAA. In the case of MAA (TS-MAA and TS-MAA-dimer) for the meso chain the *gauche* addition is preferred. In the case of AA (TS-AA and TS-AA-dimer), due to the absence of a methyl group at the alpha position which leads to steric repulsions, the *anti*-addition is preferred. These trends are dictated by steric effects as well as by long range stabilizing interactions between the carbonyl oxygen and the hydrogens of the methyl group.

AA has an earlier transition state (2.290 Å) and lower activation barrier of 6.43 kcal/mol (B3LYP/6-31+G(d)) than MAA which has a late transition state (2.256 Å) with an activation barrier of 8.81 kcal/mol (Fig. 2). Most probably these geometrical

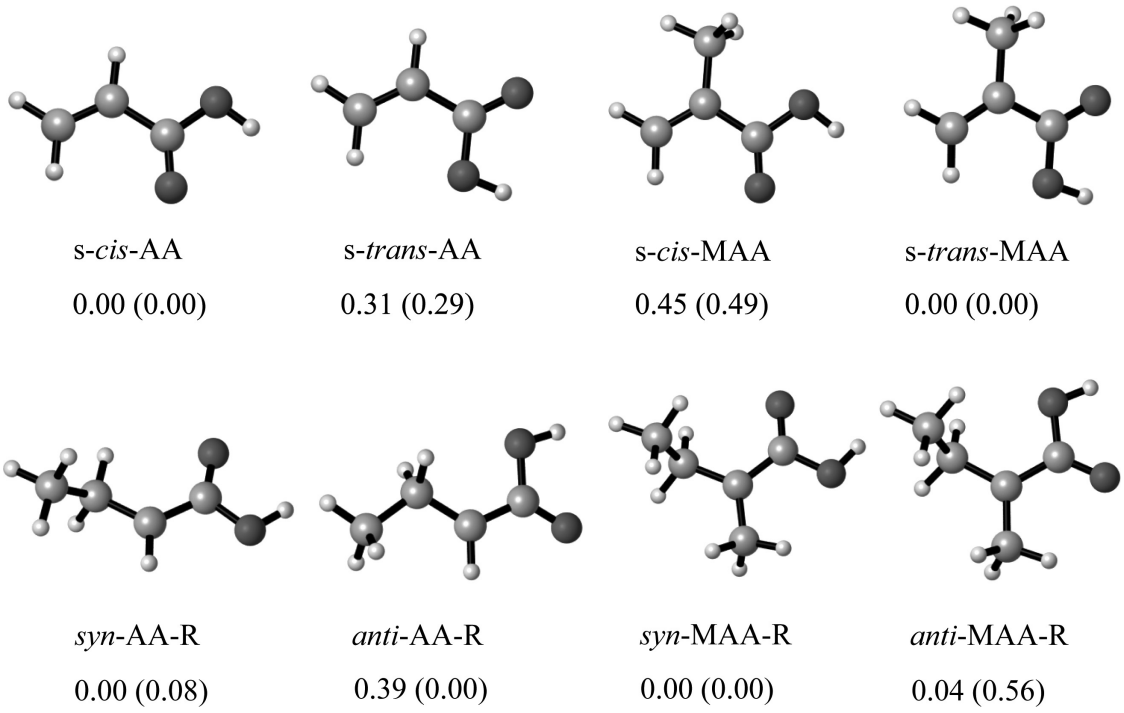

FIGURE 1 Relative electronic energies (Gibbs free energies in parenthesis) for the most stable conformers of the monomers and the radicals of AA and MAA (B3LYP/6-31+G(d)).

features can be ascribed to additional steric effects present in MAA due to the methyl group at the α position of the monomer. The early transition state and the absence of the steric group in the proximity of the reactive center lead to a higher rate for the propagation reaction in the case of AA.

The most stable transition states have been chosen (pro-racemo in case of AA and pro-meso in case of MAA) and the chains were extended to dimeric chains to mimic better the propagating radical. The dimeric transition states show similar features as compared to the unimeric model for AA with an early transition, a critical bond distance of 2.287 Å, and an activation barrier of 6.49 kcal/mol and a relatively late transition state for MAA with higher activation energy (10.37 kcal/mol) and critical bond distance of 2.225 Å (Fig. 2). As the chain extends, the activation barrier for AA does not change significantly, whereas that of MAA increases by 1.5 kcal/mol, because the radical center is even more hindered in the alpha position.

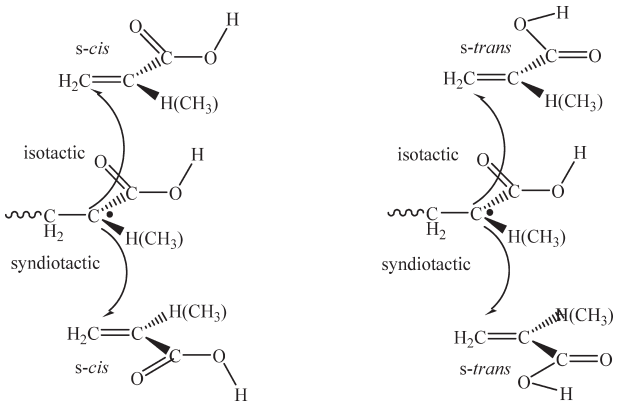

SCHEME 2 Stereoselective radical (*syn*) addition to **AA** and **MAA** (s-*cis* and s-*trans*).

We have also considered transition structures where the propagation occurs via the attack of cyclic dimers of AA and MAA. The activation barriers for the latter are slightly lower than the others in vacuum (Fig. 3, Table 2).

Propagation of AA and MAA in Solution

Molecular dynamic simulations were carried out to understand the location of water molecules around the propagating species. Thus dimeric chains of AA (HOOC—CH_2—CH_2—C(H)(CH_3)(CO—OH) and MAA (HOOC—CH(CH_3) —CH_2—C(CH_3)(CH_3)(COOH) are chosen as models for PAA and PMAA respectively and were placed separately in a box of water as described earlier. Analysis of the radial distribution functions for PAA shows that the water molecules are trapped in the vicinity of the acidic ends of the dimeric chains (Fig. 4) with the closest distance being the one between the —OH moiety of the carboxyl group of the polymeric chain and water. The radial distribution function for PMAA is shown in Supporting Information Figure S4. Almost all of the snapshots have recorded a water molecule to be within a hydrogen bond distance (1.7 Å) from the acidic proton on each end of the chain. A snapshot from the MD simulation of PAA displays the water molecules in the proximity of the acidic end (Fig. 5). In view of these results we decided to use an explicit water molecule on the polymeric chain in the proximity of the acidic functionality to mimic explicit interactions with the solvent environment of PAA and PMAA

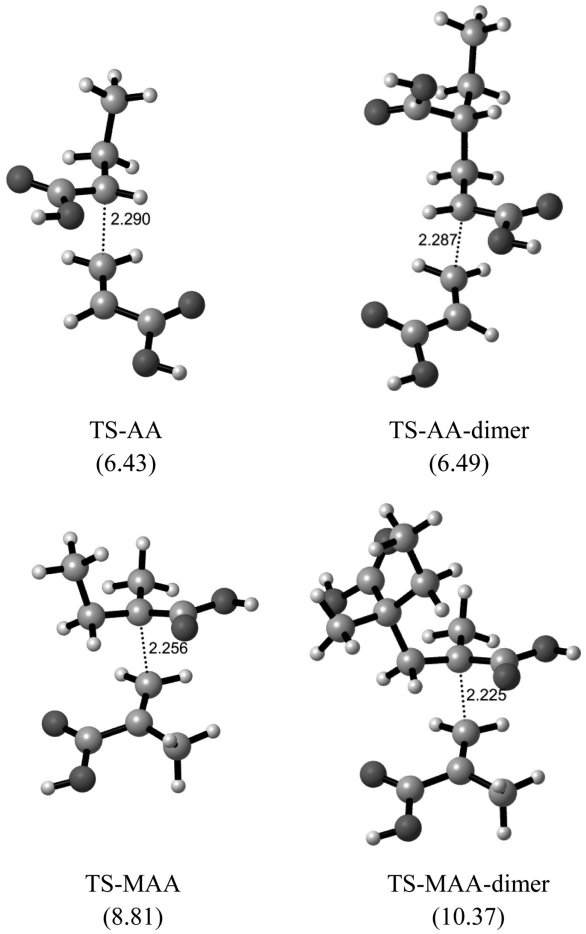

FIGURE 2 Most stable transition state structures of AA and MAA in vacuum (B3LYP/6-31+G(d)) (Electronic activation barriers are given in parenthesis (kcal/mol)).

in water. The bulk solvent effects on the geometry were further included by systematically optimizing the structures using a bulk electrostatic model (PCM), as explained in the methodology section.

We constructed unimeric and dimeric transition states by adding one explicit water molecule to each acidic end of the monomer and the radical. The optimized transition structures in implicit solvent states are depicted in Figure 6. All the transition structures with explicit water molecules have longer critical bond distances than their counterparts in vacuum, indicating slightly earlier transition structures. Note that long critical bonds lead to an increase in the disorder of the polymeric chain and thus are an indication of rate acceleration. Both for AA and MAA critical distances slightly shorten while passing from the unimeric to the dimeric case, due to an increase of steric factors.

TABLE 1 Relative Electronic Energies (ZPE included, kcal/mol) Leading to Pro-Racemo and Pro-Meso Unimeric Transition States (B3LYP/6–31+G(d))

		AA		MAA	
Stereoregularity	Radical	s-*cis*	s-*trans*	s-*cis*	s-*trans*
pro-racemo	*syn*	**0.00**[a]	0.87	0.09	0.34
pro-meso	*syn*	0.31	1.38	**0.00**[b]	0.39
pro-racemo	*anti*	0.98	1.74	0.11	0.44
pro-meso	*anti*	0.86	1.62	0.23	1.62

[a] TS-AA (pro-racemo) in Figure 2 has an electronic activation barrier of 6.43 kcal/mol (B3LYP/6–31+G(d)).
[b] TS-MAA (pro-meso) in Figure 2 has an electronic activation barrier of 8.81 kcal/mol (B3LYP/6–31+G(d)).

A general overview of the electronic activation energies for AA and MAA in the various models, using different levels of theory together with the experimental values is given in Table 2. Polymeric chains with cyclic dimers have not been observed in MD simulations with water, thus the corresponding transition structures have not been considered. For AA, the activation barrier increases slightly (0.79 kcal/mol) as passing from the gas phase to aqueous medium, whereas for MAA this change is even smaller (0.26 kcal/mol).[15,25,27] Except for the B3LYP methodology all the other functionals—MPWB1K, M05-2X, and M06-2X—predict the change in the activation barriers in the correct direction and magnitude. The experimental values are better described using a dimeric model. Note that the M06-2X functional reproduces the experimental values in solvent quite satisfactorily.

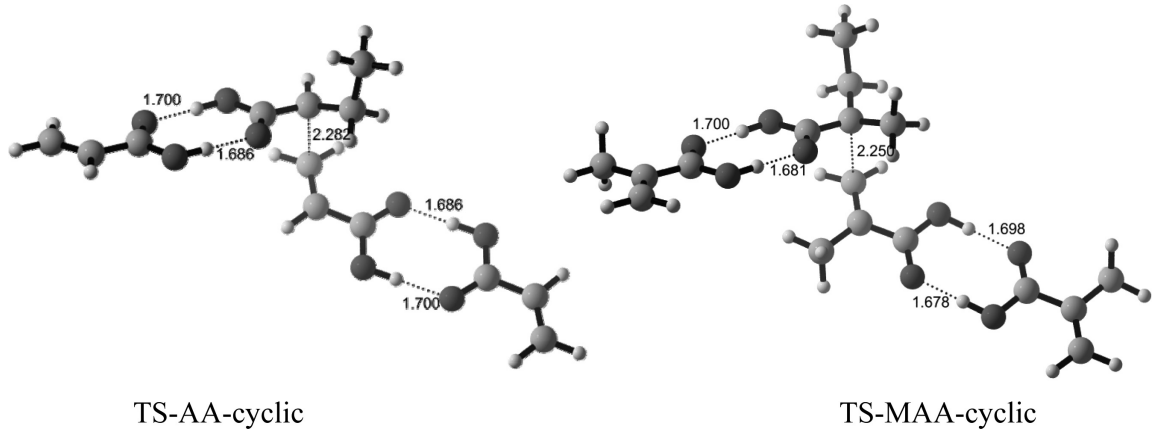

FIGURE 3 Propagation transition state structures for cyclic dimers of AA and MAA (B3LYP/6-31+G(d)).

TABLE 2 Activation Energy Barriers (kcal/mol) for the Unimeric Propagating Chains of AA and MAA

		E_{a_gas}	E_{a_water}	ΔE_a
AA	B3LYP[a]	6.43 (6.49) [*6.38*]	8.78 (9.41)	−2.35 (−2.92)
	MPWB1K[b]	5.09 (5.20) [*4.76*]	5.16 (5.53)	−0.07 (−0.33)
	M05–2X[b]	1.98 (2.23) [*1.62*]	2.08 (2.48)	−0.10 (−0.25)
	M06–2X[b]	3.02 (3.24) [*2.59*]	3.03 (3.40)	−0.01 (−0.16)
	Exp.	2.89[c]	3.68[d]	−0.79
MAA	B3LYP[a]	8.81 (10.37) [*8.61*]	11.73 (14.07)	−2.92 (−3.70)
	MPWB1K[b]	6.13 (6.86) [*5.88*]	5.20 (6.45)	0.93 (0.41)
	M05–2X[b]	2.26 (3.20) [*2.02*]	1.38 (2.77)	0.88 (0.43)
	M06–2X[b]	3.06 (3.76) [*2.61*]	1.96 (3.25)	1.10 (0.51)
	Exp.	3.85 ± 0.4[e]	3.47 ± 0.1[f]	0.26

The corresponding values for the dimers are given in parenthesis, those for the cyclic structures are displayed in brackets and italics. ΔE_a is defined as the difference between the activation barrier in gas phase ($E_{a\text{-gas}}$) and in water environment ($E_{a\text{-water}}$).
[a] Gas phase optimizations are carried out at the B3LYP/6–31+G(d) level and aqueous phase optimizations are carried out for the explicitly solvated structures by PCM methodology with B3LYP/6–31+G(d).
[b] The "Functional"/6–311+G(3df,2p)//B3LYP/6–31+G(d)-PCM methodology has been used for aqueous phase calculations.
[c] extrapolated from 40 wt % at 25 °C, Ref. 27.
[d] 10 wt % AA at 2.1–20.1 °C, Ref. 27.
[e] Extrapolated from 40 wt % at 25 °C, Ref. 25.
[f] 15 wt % MAA at 25 °C, Ref. 25.

The Gibbs Free energies of activation as well as the propagation rate constants for both monomers in bulk and water are given in Table 3 together with the experimental data. Notice that in bulk polymerization the monomer acts just as one particular solvent and that it is the difference in intermolecular interactions between the transition structure and different solvent environments which determines whether there is a solvent dependence of k_p. As the activation barriers in water and in vacuum are very close to each other (Table 2), the rate enhancement must be attributed to the increase of entropy in aqueous medium. It is worthwhile noticing that the kinetic parameters obtained with the M06-2X/6-311+G(3df,2p)//B3LYP/6-31+G(d) methodology and the dimeric model are closer to the experimental ones than those obtained with the other methodologies.

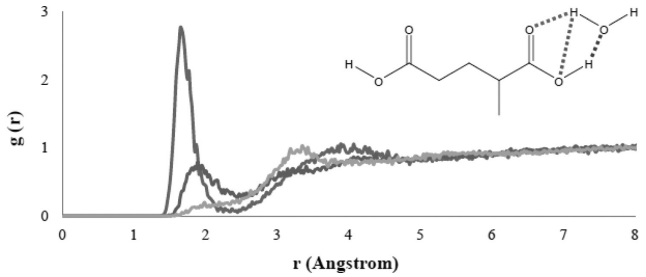

FIGURE 4 Radial distribution functions for a dimeric AA chain. The interactions between acidic protons of AA and oxygen of water are shown in blue (—); the interactions between the carbonyl oxygens of AA and the protons of water are in red (—); the interactions between the —OH oxygens of AA and the protons of the water are in green (—).

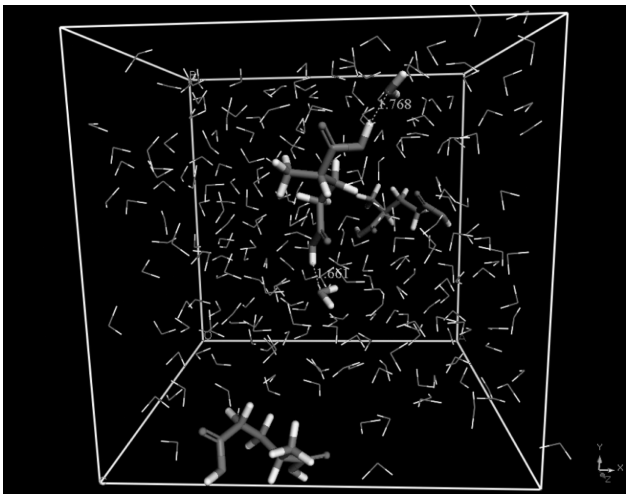

FIGURE 5 A snapshot from the MD simulation of PAA (model).

The rate acceleration of AA_{bulk} as compared to MAA_{bulk} can be attributed to the presence of the methyl group in the alpha position of MAA that hinders the radical center for further attack. A direct relationship between the reactivity and the electron density on the atoms where the reaction occurs was suggested in the work of Beuermann.[5] The solvent is expected to change the electron density of the carbon atoms of the double bond and alter the reactivity as discussed in the literature.[25] To validate this suggestion, we performed a charge analysis on the various monomers, with and without explicit solvent interactions. Based on the calculated NBO charges for the monomers and the radicals in the gas phase and in water some qualitative trends can be drawn (Fig. 7). C1 of *s-cis*-AA has a charge of −0.334, whereas C1 of ***s-trans***-MAA is −0.355; C1 of s-*cis*-AA is more electron deficient and more susceptible to be attacked by a radical. The radical center C2 (secondary radical) of *syn*-AA-R is richer in electrons as compared with the radical center of *anti*-MAA-R (tertiary radical). Overall based on the electronic charges one can predict AA to polymerize faster than MAA. In solution, the electron densities do not change much and this in agreement with our previous findings on the origin of rate acceleration in solution: rate acceleration in solution is due to a change in entropy rather than a change in electronic charges.

CONCLUSIONS

In this study, we have used static and molecular dynamics computational tools to rationalize the rate acceleration in the FRP of AA and MAA in water and assess their relative rates of polymerization. Experimentally, it was found that AA polymerizes faster than MAA both in bulk and in water. Furthermore the rate of polymerization is faster in water than in bulk both for AA and MAA. Molecular dynamics calculations were performed to understand the explicit interactions between the polymer chain and the water molecules. It was

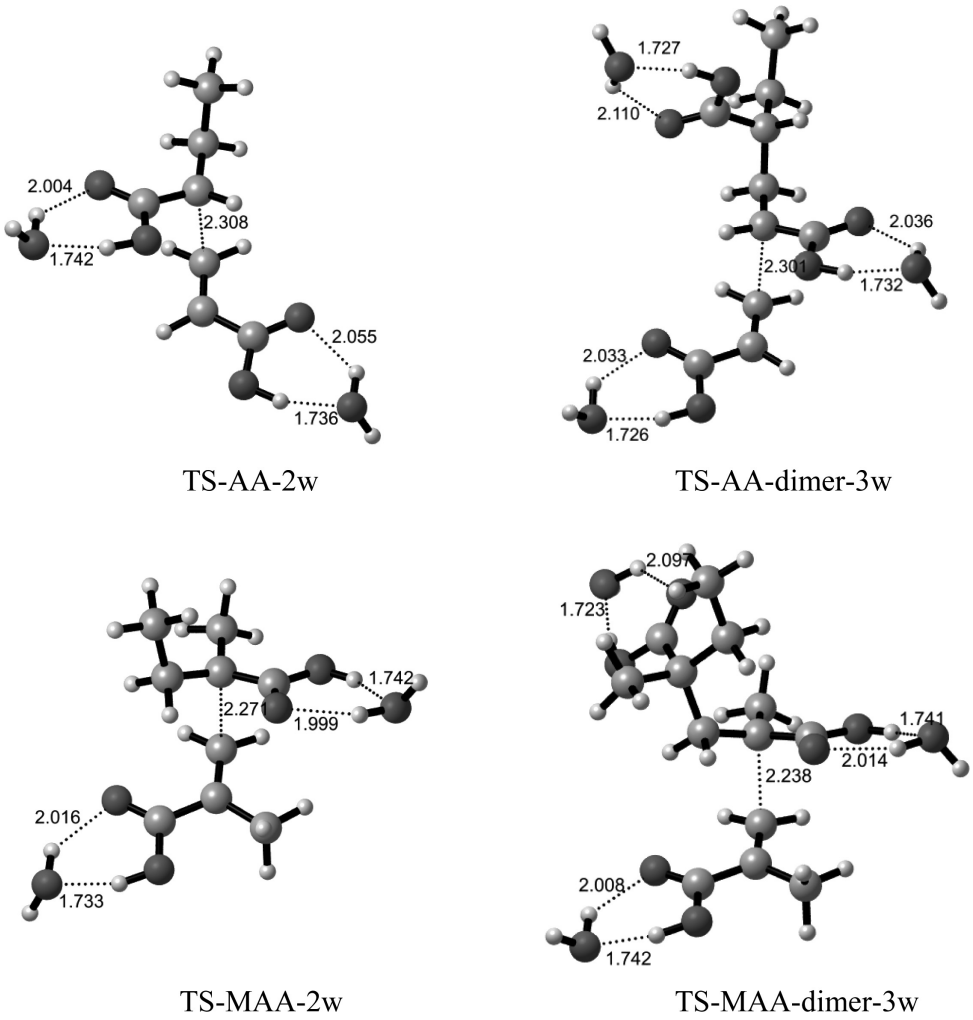

FIGURE 6 Most stable transition state structures of AA and MAA in water (B3LYP/6-31+G(d) -PCM).

TABLE 3 Gibbs Free energies of activation (25 °C, kcal/mol) and propagation rate constants k_p (L/mol·s) in bulk and aqueous media

		Bulk		Water	
		$\Delta G^{\neq}$	k_p	$\Delta G^{\neq}$	k_p
AA	MPWB1K[a]	14.53 (14.93) [*14.45*]	3.36E+03 (1.71E+03) [*3.85E+03*]	14.88 (14.70)	1.85E+03 (2.51E+03)
	M05–2X[a]	11.42 (11.95) [*11.31*]	6.37E+05 (2.60E+05) [*7.74E+05*]	11.80 (11.66)	3.35E+05 (4.27E+05)
	M06–2X[a]	12.46 (12.96) [*12.28*]	1.10E+05 (4.75E+04) [*1.51E+05*]	12.76 (12.58)	6.71E+04 (0.91E+05)
	Exp.	–	2.01E+04[b]	–	1.32E+05[c]
MAA	MPWB1K[a]	17.51 (19.23) [*15.57*]	2.21E+01 (1.20E+00) [*5.78E+02*]	16.61 (17.89)	1.01E+02 (1.16E+01)
	M05–2X[a]	13.63 (15.57) [*11.71*]	1.54E+04 (5.81E+02) [*3.91E+05*]	12.79 (16.11)	6.37E+04 (2.34E+02)
	M06–2X[a]	14.43 (16.13) [*13.67*]	3.95E+03 (2.24E+02) [*1.44E+04*]	13.37 (14.69)	2.36E+04 (2.58E+03)
	Exp.	–	5.74E+02[d]	–	3.83E+03[e]

The corresponding values for the dimers are given in parenthesis, those for the cyclic structures are displayed in brackets and italics.
[a] COSMO-RS is used for calculations in bulk, optimized structures in vacuum are used. The "Functional"/6–311+G(3df,2p)//B3LYP/6–31+G(d) methodology is used for the energetics. For the aqueous phase calculations, explicitly solvated structures are optimized with B3LYP/6–31+G(d) in a continuum (PCM), the "Functional"/6–311+G(3df,2p)//B3LYP/6–31+G(d)-PCM methodology is used for the energetics and is followed by COSMO-RS calculations in water at 25 °C.
[b] Extrapolated from 40 wt % at 25 °C, Ref. 27.
[c] 10 wt % AA in water at 2.1–20.1 °C, Ref. 27.
[d] Extrapolated from 40 wt % at 25 °C, Ref. 25.
[e] 15 wt % MAA in water at 25 °C, Ref. 25.
The sign (≠) stands for excited states (transition state).

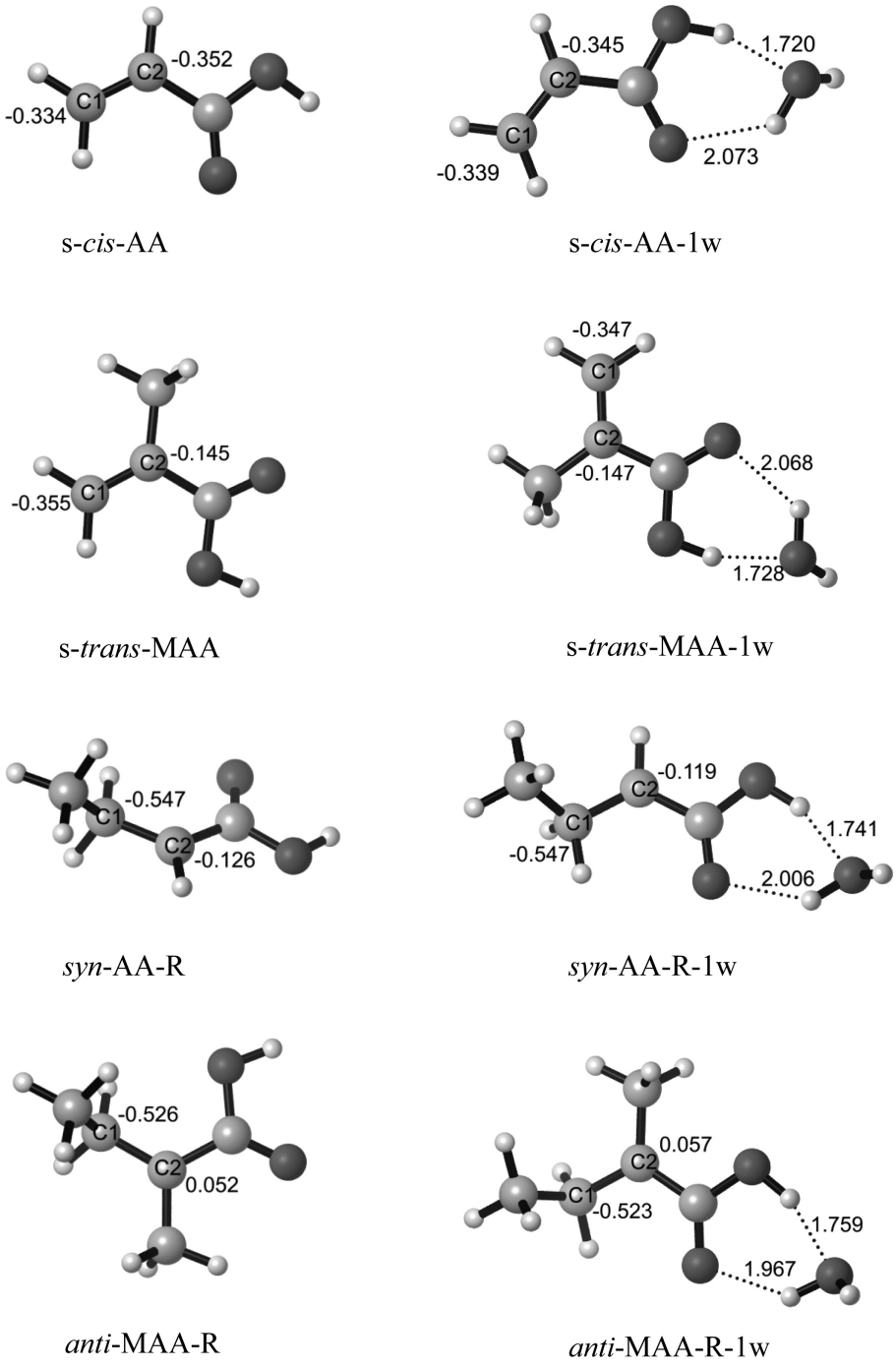

FIGURE 7 NBO charges and geometrical parameters for the monomers and radicals in vacuum and in aqueous medium (optimized in water with the PCM methodology) (B3LYP/6-31+G(d)).

found that water prefers a coordination with the carboxyl group of the propagating chains. Extensive transition state searches were performed for MAA and AA in gas phase and water environment. The slower propagation for MAA compared to AA, was ascribed to additional steric effects present in MAA due to the methyl group at the α position of the monomer in both media. In both cases, in water, the acidic end of the reacting species is captured by water. In water, the electronic distribution at the reactive centers in the transition states diminishes, the critical bonds are longer, the entropy of activation increases, the rate of propagation increases. This study emphasizes the fact that M06-2X/6-311+G(3df,2p)//B3LYP/6-31+G(d) methodology reproduces quantitatively the experimental rate accelerations of AA and MAA in water and is more suitable for modeling their FRP kinetics. Overall, quantum chemical tools have been used to enlighten the rate acceleration of the FRP of both species in water. The dimeric models and the methodology proposed in

this study can be used for further understanding of the solvent effect on the propagation kinetics of acrylate derivatives. The propagation of cyclic dimers plays also a role in the FRP kinetics of AA and MAA in bulk, conclusive results about the propagation mechanism can further be drawn by taking into consideration longer propagating chains.

ACKNOWLEDGMENTS

The computational resources used in this work were provided by Ghent University, the National Center for High Performance Computing of Turkey (UYBHM) under the grant number 20502009, the TUBITAK ULAKBIM High Performance Computing Center and the project DPT-2009K120520. The UGent authors thank the FWO (Fonds voor Wetenschappelijk Onderzoek - Vlaanderen, Fund for Scientific Research - Flanders), the research board of Ghent University for the bilateral project Ghent – Istanbul and the IAP-BELSPO project in the frame of IAP 6/27 for financial support of this research.

REFERENCES AND NOTES

1 Y. E. Kirsh, Water-Soluble Poly-N-Vinylamides: Synthesis and Physico-Chemical Properties; Wiley: Chichester, New York, **1998.**

2 S. K. Tripathy, J. Kumar, H. S. Nalwa, Handbook of Polyelectrolytes and their Applications;. Applications of Polyelectrolytes and Theoretical Models; American Scientific: Stevenson Ranch, Calif., **2002**; Vol. 3.

3 S. Beuermann, M. Buback, *Prog. Polym. Sci.* **2002,** *27*, 191–254.

4 O. F. Olaj, I. Bitai, F. Hinkelmann, *Macromol. Chem. Phys.* **1987,** *188*, 1689–1702.

5 S. Beuermann, *Macromol. Rapid Commun.* **2009,** *30*, 1066–1088.

6 S. Beuermann, D. Nelke, *Macromol. Chem. Phys.* **2003,** *204*, 460–470.

7 K. F. ODriscoll, M. L. Monteiro, B. Klumperman, *J. Polym. Sci. Part A: Polym. Chem.* **1997,** *35*, 515–520.

8 M. D. Zammit, T. P. Davis, G. D. Willett, K. F. ODriscoll, *J. Polym. Sci. Part A: Polym. Chem.* **1997,** *35*, 2311–2321.

9 S. Harrisson, Barner-C. Kowollik, T. P. Davis, R. Evans, E. Rizzardo, M. Stenzel, M. Yin, *Z. Phys. Chem.* **2005,** *219*, 267–281.

10 H. Fischer, L. Radom, *Angew. Chem. Int. Ed. Engl.* **2001,** *40*, 1340–1371.

11 S. Beuermann, M. Buback, G. T. Russell, *Macromol. Rapid Commun.* **1994,** *15*, 647–653.

12 S. Beuermann, D. A. Paquet, J. H. McMinn, R. A. Hutchinson, *Macromolecules* **1997,** *30*, 194–197.

13 T. P. Davis, K. F. Odriscoll, M. C. Piton, M. A. Winnik, *Macromolecules* **1989,** *22*, 2785–2788.

14 R. A. Hutchinson, J. R. Richards, M. T. Aronson, *Macromolecules* **1994,** *27*, 4530–4537.

15 F. D. Kuchta, van A. M. Herk, A. L. German, *Macromolecules* **2000,** *33*, 3641–3649.

16 R. A. Lyons, J. Hutovic, M. C. Piton, D. I. Christie, P. A. Clay, B. G. Manders, S. H. Kable, R. G. Gilbert, *Macromolecules* **1996,** *29*, 1918–1927.

17 B. R. Morrison, M. C. Piton, M. A. Winnik, R. G. Gilbert, D. H. Napper, *Macromolecules* **1993,** *26*, 4368–4372.

18 F. Ganachaud, R. Balic, M. J. Monteiro, R. G. Gilbert, *Macromolecules* **2000,** *33*, 8589–8596.

19 H. R. Lin, *Eur. Polym. J.* **2001,** *37*, 1507–1510.

20 P. Pascal, M. A. Winnik, D. H. Napper, R. G. Gilbert, *Macromolecules* **1993,** *26*, 4572–4576.

21 S. A. Seabrook, M. P. Tonge, R. G. Gilbert, *J. Polym. Sci. Part A: Polym. Chem.* **2005,** *43*, 1357–1368.

22 S. Beuermann, M. Buback, P. Hesse, F. D. Kuchta, I. Lacik, Van A. M. Herk, *Pure Appl. Chem.* **2007,** *79*, 1463–1469.

23 S. Beuermann, M. Buback, P. Hesse, S. Kukuckova, I. Lacik, *Macromol. Symp.* **2007,** *248*, 23–32.

24 S. Beuermann, M. Buback, P. Hesse, S. Kukuckova, I. Lacik, *Macromol. Symp.* **2007,** *248*, 41–49.

25 S. Beuermann, M. Buback, P. Hesse, I. Lacik, *Macromolecules* **2006,** *39*, 184–193.

26 I. Lacík, S. Beuermann, M. Buback, *Macromolecules* **2001,** *34*, 6224–6228.

27 I. Lacík, S. Beuermann, M. Buback, *Macromolecules* **2003,** *36*, 9355–9363.

28 I. Lacík, S. Beuermann, M. Buback, *Macromol. Chem. Phys.* **2004,** *205*, 1080–1087.

29 A. Chapiro, *Pure Appl. Chem.* **1981,** *53*, 643–655.

30 A. Chapiro, J. Dulieu, *Eur. Polym. J.* **1977,** *13*, 563–577.

31 V. F. Gromov, N. I. Galperina, T. O. Osmanov, P. M. Khomikovskii, A. D. Abkin, *Eur. Polym. J.* **1980,** *16*, 529–535.

32 K. Plochocka, *J. Macromol. Sci. Rev. Macromol. Chem. Phys.* **1981,** *C20*, 67–148.

33 M. Buback, P. Hesse, R. A. Hutchinson, P. Kasak, I. Lacik, M. Stach, I. Utz, *Ind. Eng. Chem. Res.* **2008,** *47*, 8197–8204.

34 M. Stach, I. Lacik, D. Chorvat, M. Buback, P. Hesse, R. A. Hutchinson, L. Tang, *Macromolecules* **2008,** *41*, 5174–5185.

35 M. Buback, *Macromol. Symp.* **2009,** *275–276*, 90–101.

36 M. Dossi, G. Storti, D. Moscatelli, *Macromol. Theory Simul.* **2010,** *19*, 170–178.

37 T. Furuncuoglu, I. Ugur, I. Degirmenci, V. Aviyente, *Macromolecules* **2010,** *43*, 1823–1835.

38 Gomez-R. Balderas, M. L. Coote, D. J. Henry, H. Fischer, L. Radom, *J. Phys. Chem A* **2003,** *107*, 6082–6090.

39 Gomez-R. Balderas, M. L. Coote, D. J. Henry, L. Radom, *J. Phys. Chem. A* **2004,** *108*, 2874–2883.

40 D. J. Henry, M. L. Coote, Gomez-R. Balderas, L. Radom, *J. Am. Chem. Soc.* **2004,** *126*, 1732–1740.

41 J. P. A. Heuts, R. G. Gilbert, I. A. Maxwell, *Macromolecules* **1997,** *30*, 726–736.

42 J. P. A. Heuts, R. G. Gilbert, L. Radom, *Macromolecules* **1995,** *28*, 8771–8781.

43 J. P. A. Heuts, R. G. Gilbert, L. Radom, *J. Phys. Chem.* **1996,** *100*, 18997–19006.

44 D. M. Huang, M. J. Monteiro, R. G. Gilbert, *Macromolecules* **1998,** *31*, 5175–5187.

45 E. I. Izgorodina, M. L. Coote, *Chem. Phys.* **2006,** *324*, 96–110.

46 C. Y. Lin, E. I. Izgorodina, M. L. Coote, *Macromolecules* **2010,** *43*, 553–560.

47 D. Moscatelli, M. Dossi, C. Cavallotti, G. Storti, *Macromol. Symp.* **2007,** *259*, 337–347.

48 D. Moscatelli, M. Dossi, C. Cavallotti, G. Storti, *J. Phys Chem. A* **2011,** *115*, 52–62.

49 K. Van Cauter, K. Hemelsoet, V. Van Speybroeck, M. F. Reyniers, M. Waroquier, *Int. J. Quantum Chem.* **2005,** *102*, 454–460.

50 K. Van Cauter, V. Van Speybroeck, P. Vansteenkiste, M. F. Reyniers, M. Waroquier, *Chemphyschem* **2006,** *7*, 131–140.

51 Van K. Cauter, Van V. Speybroeck, M. Waroquier, *Chemphyschem* **2007,** *8*, 541–552.

52 M. W. Wong, L. Radom, *J. Phys. Chem.* **1995,** *99*, 8582–8588.

53 M. W. Wong, L. Radom, *J. Phys Chem. A* **1998,** *102*, 2237–2245.

54 I. Degirmenci, D. Avci, V. Aviyente, K. Van Cauter, V. Van Speybroeck, M. Waroquier, *Macromolecules* **2007,** *40*, 9590–9602.

55 I. Degirmenci, V. Aviyente, V. Van Speybroeck, M. Waroquier, *Macromolecules* **2009,** *42*, 3033–3041.

56 I. Degirmenci, S. Eren, V. Aviyente, B. De Sterck, K. Hemelsoet, V. Van Speybroeck, M. Waroquier, *Macromolecules* **2010,** *43*, 5602–5610.

57 M. Dossi, K. Liang, R. A. Hutchinson, D. Moscatelli, *J. Phys. Chem. B* **2010,** *114*, 4213–4222.

58 M. Dossi, G. Storti, D. Moscatelli, *Polymer Reaction Engineering—10th International Workshop;* Hamburg, Germany; **2011,** *302*, 16–25.

59 H. Gunaydin, S. Salman, N. S. Tuzun, D. Avci, V. Aviyente, *Int. J. Quantum Chem.* **2005,** *103*, 176–189.

60 K. Liang, M. Dossi, D. Moscatelli, R. A. Hutchinson, *Macromolecules* **2009,** *42*, 7736–7744.

61 D. Moscatelli, C. Cavallotti, M. Morbidelli, *Macromolecules* **2006,** *39*, 9641–9653.

62 T. F. Ozaltin, I. Degirmenci, V. Aviyente, C. Atilgan, B. De Sterck, V. Van Speybroeck, M. Waroquier, *Polymer* **2011,** *52*, 5503–5512.

63 S. Salman, A. Z. Albayrak, D. Avci, V. Aviyente, *J. Polym. Sci. Part A: Polym. Chem.* **2005,** *43*, 2574–2583.

64 X. R. Yu, J. Pfaendtner, L. J. Broadbelt, *J. Phys Chem. A* **2008,** *112*, 6772–6782.

65 S. C. Thickett, R. G. Gilbert, *Polymer* **2004,** *45*, 6993–6999.

66 B. De Sterck, R. Vaneerdeweg, F. Du Prez, M. Waroquier, V. Van Speybroeck, *Macromolecules* **2010,** *43*, 827–836.

67 X. R. Yu, S. E. Levine, L. J. Broadbelt, *Macromolecules* **2008,** *41*, 8242–8251.

68 D. M. Smith, R. G. Lehmann, R. Narayan, G. E. Kozerski, J. R. Miller, *Compost Sci. Utilization* **1998,** *6*, 6–12.

69 P. Deglmann, I. Muller, F. Becker, A. Schafer, K. D. Hungenberg, H. Weiss, *Macromol. React. Eng.* **2009,** *3*, 496–515.

70 M. L. Coote, *Macromol. Theory Simul.* **2009,** *18*, 388–400.

71 D. J. Henry, M. B. Sullivan, L. Radom, *J. Chem. Phys.* **2003,** *118*, 4849–4860.

72 A. Klamt, COSMO-RS: From Quantum Chemistry to Fluid Phase Thermodynamics and Drug Design; Elsevier: Amsterdam, Oxford, **2005**; p xi, 34 p.

73 A. Klamt, *J. Phys. Chem.* **1995,** *99*, 2224–2235.

74 A. Klamt, V. Jonas, T. Burger, J. C. W. Lohrenz, *J. Phys Chem. A* **1998,** *102*, 5074–5085.

75 S. C. L. Kamerlin, M. Haranczyk, A. Warshel, *Chemphyschem* **2009,** *10*, 1125–1134.

76 M. J. Pilling, P. W. Seakins, Reaction Kinetics; Oxford University Press: Oxford, **1995**; p xiii, 305p.

77 M. L. Coote, T. P. Davis, L. Radom, *Macromolecules* **1999,** *32*, 5270–5276.

78 M. L. Coote, T. P. Davis, L. Radom, *Macromolecules* **1999,** *32*, 2935–2940.

79 M. J. T. Frisch, G. W. Trucks, H. B. Schlegel, G. E. Scuseria, M. A. Robb, J. R. Cheeseman, J. A. Montgomery Jr., T. Vreven, K. N. Kudin, J. C. Burant, J. M. Millam, S. S. Iyengar, J. Tomasi, V. Barone, B. Mennucci, M. Cossi, G. Scalmani, N. Rega, G. A. Petersson, H. Nakatsuji, M. Hada, M. Ehara, K. Toyota, R. Fukuda, J. Hasegawa, M. Ishida, T. Nakajima, Y. Honda, O. Kitao, H. Nakai, M. Klene, X. Li, J. E. Knox, H. P. Hratchian, J. B. Cross, V. Bakken, C. Adamo, J. Jaramillo, R. Gomperts, R. E. Stratmann, O. Yazyev, A. J. Austin, R. Cammi, C. Pomelli, J. W. Ochterski, P. Y. Ayala, K. Morokuma, G. A. Voth, P. Salvador, J. J. Dannenberg, V. G. Zakrzewski, S. Dapprich, A. D. Daniels, M. C. Strain, O. Farkas, D. K. Malick, A. D. Rabuck, K. Raghavachari, J. B. Foresman, J. V. Ortiz, Q. Cui, A. G. Baboul, S. Clifford, J. Cioslowski, B. B. Stefanov, G. Liu, A. Liashenko, P. Piskorz, I. Komaromi, R. L. Martin, D. J. Fox, T. Keith, Al-M. A. Laham, C. Y. Peng, A. Nanayakkara, M. Challacombe, P. M. W. Gill, B. Johnson, W. Chen, M. W. Wong, C. Gonzalez, and J. A. Pople; Gaussian 03. Revision D.01; Gaussian. Inc.: Wallingford CT, **2004.**

80 D. M. Smith, A. Nicolaides, B. T. Golding, L. Radom, *J. Am. Chem. Soc.* **1998,** *120*, 10223–10233.

81 J. N. P. Louwen, C.; E. V. Lenthe, ADF2008.01 COSMO-RS, SCM, Theoretical Chemistry; Vrije Universiteit: Amsterdam, The Netherlands, **2008.**

82 Y. Zhao, D. G. Truhlar, *J. Phys. Chem. A* **2004,** *108*, 6908–6918.

83 Y. Zhao, N. E. Schultz, D. G. Truhlar, *J. Chem. Theory Comput.* **2006,** *2*, 364–382.

84 Y. Zhao, D. G. Truhlar, *Theoret. Chem. Acc.* **2008,** *120*, 215–241.

85 G. Black, J. M. Simmie, *J. Comput. Chem.* **2010,** *31*, 1236–1248.

86 A. Galano, *Phys. Chem. Chem. Phys.* **2011,** *13*, 7147–7157.

87 A. Galano, J. R. Alvarez-Idaboy, *Org. Lett.* **2009,** *11*, 5114–5117.

88 A. Galano, N. A. Macias-Ruvalcaba, O. N. M. Campos, J. Pedraza-Chaverri, *J. Phys. Chem. B* **2010,** *114*, 6625–6635.

89 T. T. Gao, J. M. Andino, J. R. Alvarez-Idaboy, *Phys. Chem. Chem. Phys.* **2010,** *12*, 9830–9838.

90 C. Iuga, J. R. Alvarez-Idaboy, A. Vivier-Bunge, *J. Phys Chem. A* **2011,** *115*, 5138–5146.

91 Leon-J. R. Carmona, A. Galano, *J. Phys. Chem. B* **2011,** *115*, 4538–4546.

92 A. Perez-Gonzalez, A. Galano, *J. Phys. Chem. B* **2011,** *115*, 1306–1314.

93 A. Vega-Rodriguez, J. R. Alvarez-Idaboy, *Phys. Chem. Chem. Phys.* **2009,** *11*, 7649–7658.

94 E. Velez, J. Quijano, R. Notario, E. Pabon, J. Murillo, J. Leal, E. Zapata, G. Alarcon, *J. Phys. Org. Chem.* **2009,** *22*, 971–977.

95 C. Zavala-Oseguera, J. R. Alvarez-Idaboy, G. Merino, A. Galano, *J. Phys Chem. A* **2009,** *113*, 13913–13920.

96 Y. Zhao, D. G. Truhlar, *J. Chem. Theory Comput.* **2007,** *3*, 289–300.

97 D. A. McQuarrie, J. D. Simon, Physical Chemistry: A Molecular Approach; University Science Books: Sausalito, Calif., **1997**; p xxiii, 1270p.

98 P. W. Atkins, De J. Paula, Atkins' Physical Chemistry, 8th ed.; Oxford University Press: Oxford, New York, **2006**; p xxx, 1064 p.

99 E. Cances, B. Mennucci, J. Tomasi, *J. Chem. Phys.* **1997,** *107*, 3032–3041.

100 B. Mennucci, E. Cances, J. Tomasi, *J. Phys. Chem. B* **1997,** *101*, 10506–10517.

101 B. Mennucci, J. Tomasi, *J. Chem. Phys.* **1997,** *106*, 5151–5158.

102 J. Tomasi, B. Mennucci, E. Cances, *J. Mol. Struct. (Theochem)* **1999,** *464*, 211–226.

103 B. De Sterck, V. Van Speybroeck, S. Mangelinckx, G. Verniest, N. De Kimpe, M. Waroquier, *J. Phys Chem. A* **2009,** *113*, 6375–6380.

104 C. P. Kelly, C. J. Cramer, D. G. Truhlar, *J. Chem. Theory Comput.* **2005,** *1*, 1133–1152.

105 C. P. Kelly, C. J. Cramer, D. G. Truhlar, *J. Phys Chem. A* **2006,** *110*, 2493–2499.

106 Van V. Speybroeck, K. Moonen, K. Hemelsoet, C. V. Stevens, M. Waroquier, *J. Am. Chem. Soc.* **2006,** *128*, 8468–8478.

107 M. D. Liptak, K. C. Gross, P. G. Seybold, S. Feldgus, G. C. Shields, *J. Am. Chem. Soc.* **2002,** *124*, 6421–6427.

108 D. N. Theodorou, U. W. Suter, *Macromolecules* **1985,** *18*, 1467–1478.

109 H. Sun, *J. Phys. Chem. B* **1998,** *102*, 7338–7364.

110 H. C. Andersen, *J. Chem. Phys.* **1980,** *72*, 2384–2393.